# Adapting Raman Spectra from Laboratory Spectrometers to Portable Detection Libraries

**James C. Weatherall,[a,*] Jeffrey Barber,[a] Carolyn S. Brauer,[b,†] Timothy J. Johnson,[c] Yin-Fong Su,[c] Christopher D. Ball,[d] Barry T. Smith,[e] Rick Cox,[f] Robert Steinke,[f] Patricia McDaniel,[g] Louis Wasserzug[g]**

[a] *Battelle Memorial Institute, 2900 Fire Road, Egg Harbor Township, NJ 08234 USA*
[b] *Oak Ridge Institute for Science and Education, Oak Ridge, TN 37831 USA*
[c] *Pacific Northwest National Laboratory, Richland, WA 99354 USA*
[d] *Battelle Memorial Institute, 505 King Avenue, Columbus, OH 43201 USA*
[e] *U.S. Department of Homeland Security, Science and Technology Directorate, Transportation Security Laboratory, Atlantic City International Airport, NJ 08405 USA*
[f] *DeltaNu Inc., 5452 Aerospace Drive, Laramie, WY 82070 USA*
[g] *Technical Support Working Group, Combating Terrorism Technical Support Office, 4800 Mark Center Drive, Alexandria, VA 22350 USA*

**Raman spectral data collected with high-resolution laboratory spectrometers are processed into a format suitable for importing as a user library on a 1064 nm DeltaNu first generation, field-deployable spectrometer prototype. The two laboratory systems used are a 1064 nm Bruker Fourier transform (FT)-Raman spectrometer and a 785 nm Kaiser dispersive spectrometer. The steps taken to adapt for device-dependent spectral resolution, wavenumber shifts between instruments, and relative intensity response are described. Effects due to the differing excitation laser wavelengths were found to be minimal, indicating—at least for the near-infrared (NIR)—that data can be ported between different systems, so long as certain measures are taken with regard to the reference and field spectra.**

Index Headings: **Raman spectroscopy; Raman libraries; Portable; Spectral Database; Wavenumber calibration; Intensity correction; Fluorescence; Explosives Detection.**

## INTRODUCTION

Raman spectroscopy is a highly selective technique for the identification of explosives and precursor chemicals, and commercially available portable Raman units have found effective use by first responders and by the military.[1–5] Raman spectrometers identify materials by comparing field-collected spectra with "library" spectra, so the library database is critical to the effectiveness of these instruments. These libraries, and the comparison algorithms used for material identification, are developed independently for each instrument in part to accommodate differences in spectrometer design, étendue, grating, and detecting element (such as charge-coupled device [CCD] detectors), that cause Raman spectra to be device-dependent. Because of the single-beam nature of the data collection, the spectra are not self-ratioing in the sense of transmission or absorption data, and the intensities all depend on the relative response of the spectrometer. Because the libraries are device-dedicated, libraries on multiple systems need to be updated to respond to an emerging threat.[6–9] This updating causes redundancies in effort and expense that can affect response time and brings additional burdens associated with security, safety, and property rights. An alternative approach would be to make use of spectral data collected for this purpose in a standardized manner at a central facility (e.g., a government laboratory), if these data could be used in portable libraries.[10,11]

The approach described here requires matching spectra from two instruments and involves issues familiar to spectral calibration. In principle, Raman reference spectra can be acquired with calibration of the wavenumber axis and either absolute-response or relative-response calibration on the intensity axis so as to make spectra entirely portable between any system.[8,10–17] Considerable work on spectral standardization has been applied to improve long-term data archiving of reference libraries.[9] However, although long-term data archiving of Raman spectra is making progress toward developing transferable Raman spectral libraries,[6,9,10] these libraries are only now being adapted to handheld systems. The main difficulty is that handheld instruments use NIR lasers, and compact dispersive spectrometers with fast optics, and they are very susceptible to wavenumber calibration problems and relative intensity response, especially for small Raman wavenumber shifts. Also, American Society for Testing and Materials (ASTM) standards on spectral archiving have not encompassed peak shape and (relative) peak height, both of which are important to spectral comparison and change with spectrometer resolution and laser wavelength.[9,18] The approach taken here, therefore, is to apply an instrument-to-instrument mapping. A similar methodology has been used to correct Fourier transform infrared spectroscopy (FT-IR) libraries based on transmission spectra for attenuated total reflection (ATR) sampling.[19‡] A procedure is described for manipulating the spectra collected on a high-resolution laboratory instrument so as to emulate how the spectra would appear on a low-resolution field-deployed unit. This article describes effective methods as to how higher resolution spectra can be converted into lower resolution spectra; how wavenumber axis-stretching can be corrected; and how relative intensity amplitudes can be corrected, to make spectra as congruent as possible between two instruments. Issues of fluorescence and laser wavelength

---

Received 8 June 2012; accepted 21 September 2012.

* Author to whom correspondence should be sent. E-mail: weatherallj@battelle.org.

† Present address: Pacific Northwest National Laboratory, Richland, WA 37831 USA

DOI: 10.1366/12-06759

‡ R.L. Green, Thermo Fisher, Inc. Private Communication, 2011.

0003-7028/13/6702-0149/0

are addressed. The mapping applies direct instrument-to-instrument corrections, rather than standardization techniques in which each instrument is corrected to external standards;[11] this approach makes the procedure easy to implement, without intermediate calibration that is immaterial to the vendor or to the end library user, and need only be done once for each system.

In this work, two laboratory systems are used to collect reference spectra that are incorporated into two user libraries on a field-deployable spectrometer. The laboratory spectra used for this study were taken at the Pacific Northwest National Laboratory (PNNL) and at the Transportation Security Laboratory (TSL), the latter of which is part of the Department of Homeland Security, Science and Technology Directorate. These two laboratory systems operate at different illuminating laser wavelengths, and they have different spectral resolution. The PNNL system is a commercial FT-Raman system with a 1064 nm CW excitation laser,[10] whereas the Raman spectrometer used by the TSL is a commercial dispersive system with a 785 nm laser. The field-deployable spectrometer is a prototype, first generation 1064 nm system provided by DeltaNu for this research project. (Note: Reference herein to any specific commercial products, processes, equipment, or services does not constitute or imply its endorsement, recommendation, or favoring by the U.S. Government or the Department of Homeland Security, or any of its employees or contractors.)

## RAMAN SPECTROMETERS

The PNNL laboratory system is a Bruker-IFS 66v/S FT-IR spectrometer with a Bruker FT-Raman Accessory.[10,20,21] The Raman excitation source is a 1064 nm Nd:YAG laser, a germanium/calcium fluoride (Ge/$CaF_2$) beam splitter, and a single element nitrogen-cooled Ge detector. Metadata embedded in the spectra files document the instrumental parameters associated with the spectral data. Data are collected with the Bruker system typically using between 200 and 1000 mW of laser power. The instrumental resolution is set to 2.0 $cm^{-1}$ and spectral range from 101 to 3500 $cm^{-1}$ Raman shift. Due to digital zerofilling before the FT process,[10] the spectra have 14 092 points, with digital wavenumber spacing of 0.24 $cm^{-1}$. Details of the PNNL 1064 system and parameters used to collect the data are described in a separate article.[10] Extensive efforts are made to calibrate the wavelength axis, both of the interferometer and that due to the Raman laser frequency drift. These data also are corrected for relative wavelength-dependent intensity response.[12] Although not absolute cross sections, intensity-calibrated data are portable to other systems.[8]

The TSL system is a Kaiser Raman RXN1 spectrometer.[22] The Kaiser uses a 785 nm NIR gallium arsenide (GaAs) diode as the laser source, with a variable power output of 10–400 mW. Spectral coverage is from 100 to 3450 $cm^{-1}$ Raman shift, with resolution of 5 $cm^{-1}$. The Analytical Sample Compartment (HLSC) used to collect the spectra incorporates an MK II filtered fiber optic probe head. The spectra have 11 557 points, with wavenumber spacing of 0.30 $cm^{-1}$. The Kaiser uses volume-phase holograms to perform filtering and dispersion functions, in an axial transmissive spectrograph configuration. The spectrum is obtained with a fixed transmission grating on two wavenumber-shift stripes on a Si CCD detector. The grating has a 90° fold between the incident and diffracted light at the central wavelength, so that the lens can be placed very close to the grating, resulting in low f-ratio (f/1.8) and minimal vignetting. A calibration system, integrated in the HLSC, provides wavelength and intensity reference lamps. The wavelength is calibrated in an automated procedure using a spectrum of atomic emission lines produced with a neon lamp.[13,14] Intensity calibration is accomplished using the continuous spectral output of a tungsten–halogen lamp that is factory-calibrated and referenced to an NIST source.

The two laboratory reference libraries were prepared for a prototype 1064 nm DeltaNu system. The resolution of this system is lower, on the order of 14 $cm^{-1}$. The DeltaNu spectra have 2001 points, defined with integral intensities at integral wavenumber steps; excluding padding at low and high wavenumbers, the DeltaNu spectra cover the range 300–1850 $cm^{-1}$. The wavenumber calibration is set and verified using a polystyrene sample, but the detector response is not calibrated for intensity. Spectra saved as text files appear in columnar format, and a "library builder" program on the DeltaNu controlling computer moves spectral files stored in text format into user-defined libraries.

## EXPERIMENTAL

The algorithm to map the spectra from the laboratory systems onto the DeltaNu was developed by comparing spectra taken on a variety of materials with both spectrometers. Comparison was made with respect to Raman line shift, line amplitude, and line width. The data processing that determines these parameters and the study that defines the mapping algorithm are described below.

**Data Processing.** Materials used in the mapping study included acetone, acetonitrile, potassium perchlorate, sodium perchlorate, and military C-4. Potassium perchlorate ($KClO_4$) was chosen because of its narrow linewidths. Differences in spectra acquired by the laboratory and DeltaNu spectrometers are illustrated in Fig. 1 using $KClO_4$ from the Bruker spectrometer as an example. Most obvious are differences in baseline and relative peak heights, but there are also small differences in wavenumber position of the peaks, especially at low Raman shift. Although the large amplitude variation can be attributed to the uncalibrated intensity response, some differences in lineshape and amplitude are associated with the lower resolution of the portable system.

There are several factors that enter into how field spectra and library spectra are compared for identification. For example, the correspondence in wavenumber positions of the Raman lines is undoubtedly a key quantitative factor in detection algorithms.[23,24] Relative peak amplitudes are also signatures, although peak amplitude can be affected by the presence of fluorescence or other backgrounds. Changes in spectral broadening affect the library comparison as well. Thus, to obtain optimal mapping of lab data, peak positions, peak amplitudes, and linewidths should be as close as possible to what would be collected with the portable unit.

Detection algorithms on field-deployable spectrometers can be implemented in several different ways.[23,25,26] The DeltaNu prototype uses an algorithm similar to the Euclidean distance algorithm, except the unknown and the library data are centered about their respective means before the vector dot products are calculated. The mean centering of a spectrum $a$, characterized as a vector of length $n$ equal to the number of wavelength channels, is defined as

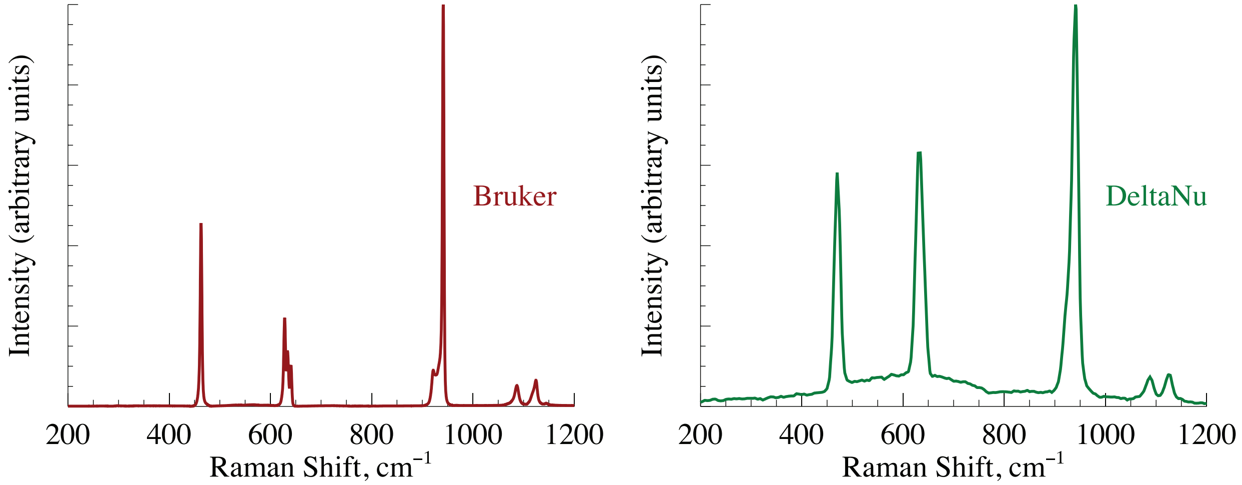

FIG. 1. Raman spectra of potassium perchlorate collected by PNNL/Bruker and DeltaNu spectrometers. The spectra are scaled to a maximal peak height at 941 cm$^{-1}$.

$$a'_m = a_m - \frac{1}{n}\sum_{i=1}^{n} a_i. \tag{1}$$

The comparison between a library entry *Lib* and the unknown spectrum *Unkn* returns a hit quality index (HQI) calculated as

$$\frac{(Lib'_m \cdot Unkn'_m)^2}{(Lib'_m \cdot Lib'_m)(Unkn'_m \cdot Unkn'_m)}. \tag{2}$$

Here, the subscript $m$ indicates the $m$th element of the spectrum, and the vector dot product is an implied sum over all the elements. The significance of the mean centering step is to make the HQI independent of the normalization of the spectra. An HQI of unity is an optimum match; a score of 0 indicates no match.

In analyzing spectra, we use spectral software to automatically identify peaks and associated wavenumbers in the Bruker/PNNL, Kaiser/TSL, and DeltaNu spectra of the mapping-study materials. The software is R-Language code, an open source statistical and graphics computing software.[27] The R-Language library *baselineWavelet* uses a function *identifyMajorPeaks* to identify the intensities and Raman shifts of Raman lines. Baseline correction is part of the peak identification and is done by wavelet and Whittaker Smooth algorithms.[28] These processes are illustrated in Fig. 2. An advantage to this method is that spectral shape is preserved, unlike derivatives or subtraction methods that change the shape of the spectrum.

An alternative method to the wavelet technique is to fit each line shape to an idealized line profile. Because most of the line broadening is in fact due to the instrumental response function, and the fit is applied to the core of the line, a Gaussian function makes a very good approximation to the observed line profile. Peak positions and amplitudes derived from the Gaussian-fitting method were used in the Kaiser conversion. We find that the data derived from the wavelet and the Gaussian-fitting methods provide similar results, with variances $\leq 2$ cm$^{-1}$ in Raman shift and $\leq 3\%$ in amplitude. These numbers are indicative of the measurement precision of line positions and amplitudes of the DeltaNu system. There are also other methods that can be used to fit the line position, such as Gaussian apodization and polynomial fitting.[13]

The mapping analysis used selected lines from the mapping study materials that covered a broad range of Raman shifts from 200 to 1800 cm$^{-1}$. Lines were selected that were simple in shape and well above the background. Sixty-four lines were used in the Bruker mapping, and 36 lines were used in the Kaiser mapping.

Although the analysis of Raman spectra focuses on scattering peaks of inherently narrow linewidth, other features in the spectra have adverse effect. It is generally recognized that removal of baseline components in the spectrum facilitates the identification of Raman lines, and there are multiple algorithms for removing baseline components.[2,23,25,29] Baseline removal would compensate for fluorescence, which is not a fixed component of the spectrum, and can vary with laser power and other instrumental settings. If the baseline is not removed as part of the library and spectral processing, it is mitigated by the detection algorithm in most cases.

Because of the 785 nm laser excitation wavelength, the Kaiser spectra are more susceptible to fluorescence than either the Bruker or the DeltaNu, both of which excite at 1064 nm.[12,18] To investigate the possibility as to whether removing fluorescent artifacts from the Kaiser spectra could improve the adapted spectra, two DeltaNu libraries were generated: one library used the "uncorrected" Kaiser spectra, and the second library used "baseline corrected" spectra in which the background is removed with the *baselineWavelet* routines. The relative performance of these libraries is a test whether baseline removal is important to the spectral mapping. The mapping algorithm that is applied to spectral conversion is described next.

## SPECTRAL MAPPING

The conversion of the laboratory spectral data into DeltaNu spectra includes the following spectral corrections:

(1) resolution smoothing (de-resolving spectra) to compensate for differences in system resolutions;
(2) wavenumber stretching to compensate for differences in peak locations;

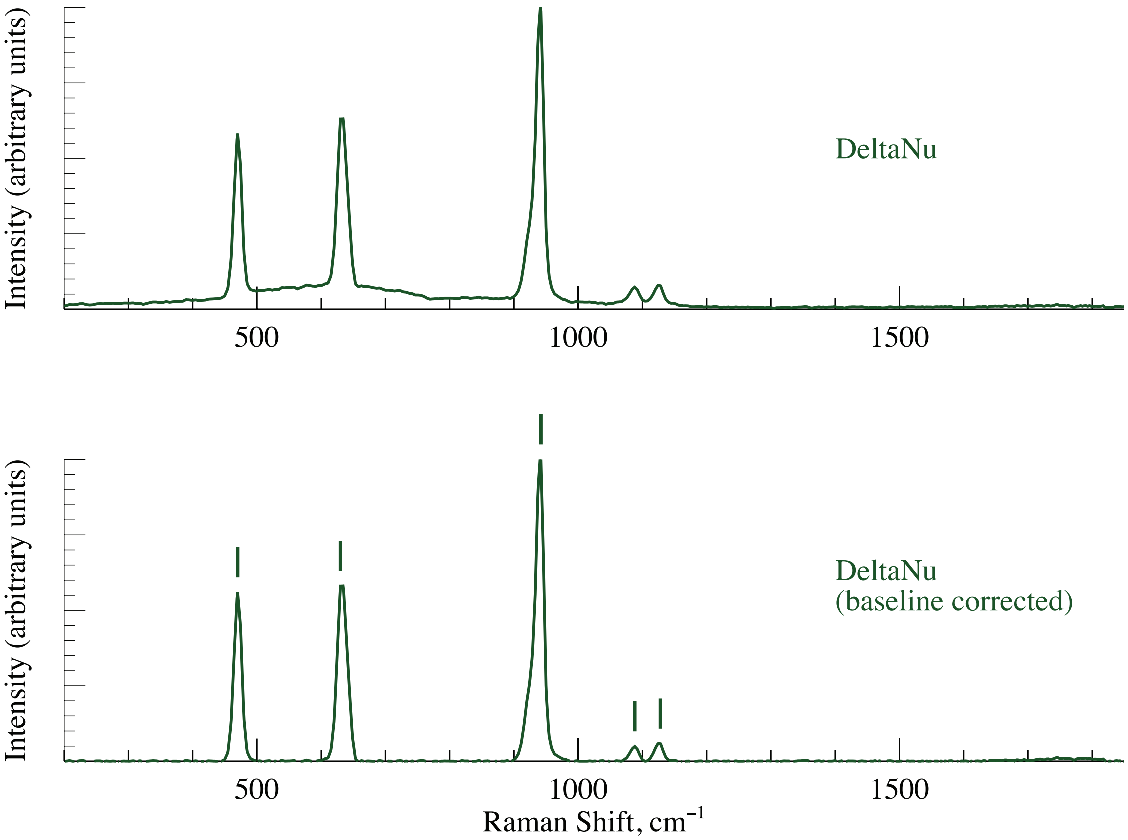

FIG. 2. The DeltaNu Raman spectrum of potassium perchlorate (top) is processed by wavelet and Whittaker Smooth algorithms to correct the baseline (bottom). The markers indicate peak locations as identified by the wavelet analysis.

(3) intensity amplitude correction to compensate for systematic differences in peak heights; and
(4) interpolation to sample the laboratory spectra at the same Raman shift wavenumbers as the DeltaNu system, i.e., grid raster matching.

**Resolution Broadening.** As the reference spectra are inherently designed to have higher resolution than the library of the portable system,[10] the spectra need to be broadened to match the instrument lineshape and width of the handheld system. This broadening is accomplished by convolution with a Gaussian kernel function. Consider a spectrum as a list (or vector) of values $a$, where the value of the $s$th element is $a_s$. Use is made of the Mathematica function *ListConvolve*,[30] a function that convolves the vector $a$ with a kernal function $K$, in this case a 121-element vector (with length determined by the wavenumber sampling of the reference spectrometer). The elements of $K$ are indexed with the first element being −60 and the last element being 60. Then, the convolved spectrum is $a'_s$,

$$a'_s = \sum_r K_r a_{s+r} \tag{3}$$

where the summation occurs over $-60 \leq r \leq 60$ (without extending past the end of the list). The kernel is given by

$$K_r = \frac{e^{-(r-1)^2/2\Delta^2}}{\sum_n e^{-(n-1)^2/2\Delta^2}} \tag{4}$$

The kernel parameter $\Delta$ corresponds to the Gaussian width of the kernel function (such that the full width at half maximum is $\mathrm{FWHM} = 2\sqrt{2\,ln(2)\Delta}$). The kernel width is dimensionless in this form, but it can be expressed in physical units by multiplying by the wavenumber spacing $\epsilon$ of the laboratory spectrum. The effect of the convolution of the laboratory spectrum with the kernel function is to broaden the laboratory spectrum to a linewidth $\delta k'_{lab} = (\delta k^2_{lab} + \Delta^2\epsilon^2)^{1/2}$. The kernel parameter is derived by finding the $\Delta$ that provides the best match of $\delta k'_{lab}$ to the DeltaNu linewidth for the set of mapping study lines. The experimental results for matching the two laboratory instruments to the handheld DeltaNu are summarized in Table I; the Bruker values are broadened by an additional amount $\Delta \times \epsilon \sim 5.3$ cm$^{-1}$ and the Kaiser by 1.6 cm$^{-1}$, and these values are commensurate with the inherent resolutions of the two laboratory systems.

**Raman Shift Correction.** Wavenumber calibration of dispersive Raman spectrometer is notoriously difficult,[3,13–15,21] particularly for handheld systems that have high étendues, i.e., light dispersed over very short distances onto array detector devices; the distortions are typically extreme at low wavenumber shifts. Systematic differences in the Raman shift

**TABLE I. Resolution correction parameters.**

| Spectrometer | Kernel $\Delta$ | Sampling Interval $\epsilon$ |
|---|---|---|
| Bruker | 22 | 0.24 cm$^{-1}$ |
| Kaiser | 5.2 | 0.30 cm$^{-1}$ |

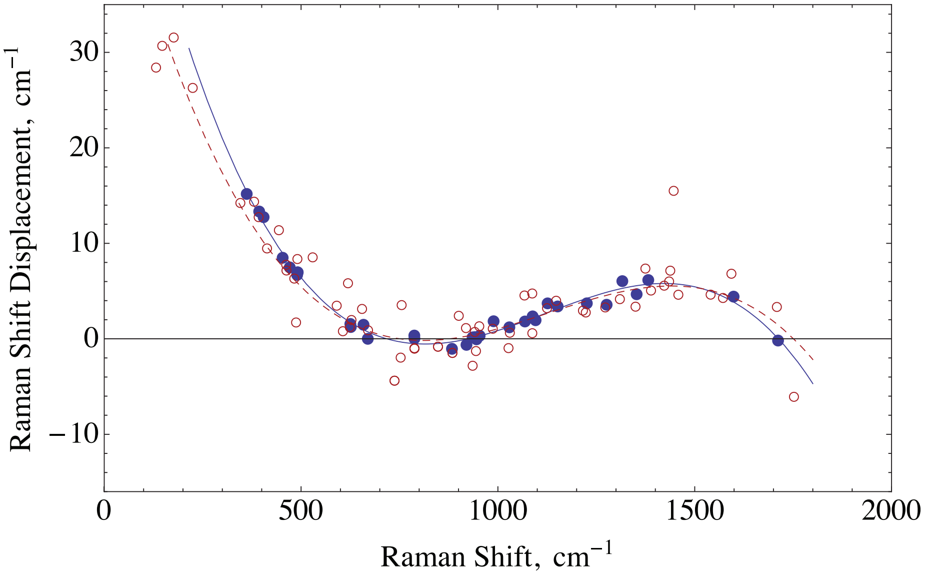

FIG. 3. Displacement in measured Raman shift in DeltaNu spectra relative to Bruker (open circles) and Kaiser (filled circles) spectra as a function of Raman shift. The dashed and solid lines are polynomial fits to Bruker and Kaiser displacements, respectively.

are found between the laboratory spectra and the DeltaNu spectra, as seen in Fig. 3, that plots the wavenumber displacement as a function of wavenumber. The wavenumber correction is indeed significant at low wavenumber, with a Raman shift correction $>15\ \mathrm{cm}^{-1}$ at Raman shift of $400\ \mathrm{cm}^{-1}$, and even more correction at very low Raman shifts. In part, the divergence at the edges of the spectrum is because the DeltaNu calibration is limited to polystyrene peaks; for example, the lowest wavenumber peak used is at $620\ \mathrm{cm}^{-1}$ Raman shift, and the calibration is extrapolated to the lower values.

A linear regression analysis to third order in Raman shift wavenumber $k$ characterizes the Raman shift correction:

$$k_{\Delta Nu} - k_{lab} = a_{lab} + b_{lab}k + c_{lab}k^2 + d_{lab}k^3 \tag{5}$$

The subscript “lab” on the wave shift coefficients represents either “Bruker” or “Kaiser.” The $p$-value statistic supports the statistical significance of the third order fit: in particular, increasing to fourth order in $k$ leads to poor $p$-values. The results of the regression analysis are given in Table II. Error in the last digit of each coefficient is given in parentheses. The wavenumber scaling from the laboratory spectra to the DeltaNu adapted spectra is accomplished by adding the corrections as specified in Eq. 5 to the spectral wavenumbers of each laboratory spectrum. The error remaining in the wavenumber-shift displacement after the correction (i.e., the vertical spread around the fitting function) is consistent with the wavenumber resolution of the systems. In effect, Eq. 5 is a calibration, and the wavenumber-shift displacement is the x-axis linearization.

**Amplitude Scaling.** In a similar manner, Fig. 4 illustrates the amplitude ratios of the DeltaNu to the two laboratory spectrometers for the lines in the mapping study.[8,21] There is an evident large systematic variation in line amplitude ratio as a function of Raman shift between the DeltaNu and laboratory spectrometers, as seen, for example, by the scaling factor of 3 to 4 needed at Raman shift of $1400\ \mathrm{cm}^{-1}$, and whose relative effect also is seen in Fig. 1. The likely explanation for the large disparity in photoresponse between the portable and the laboratory systems is a combination of vignetting in the portable instrument and the wavelength-dependent response of the detecting elements. The FT system (Bruker) does not have vignetting, and vignetting in the Kaiser system is minimal because it is a laboratory spectrometer with relatively large focal ratio. It is interesting that there is less variation associated with laser excitation than there is in the photoresponse differences among the spectrometers. Although one is a 1064 nm FT system with single element Ge detector and the other is a 785 nm dispersive system with a Si CCD detector bank, the intensity correction curves from the PNNL and TSL reference systems to the DeltaNu system follow each other closely. The Bruker and Kaiser systems are both response-corrected, whereas the DeltaNu is not: this difference suggests that intensity calibration compensates for much of the instrumental disparity, and the large amplitude variance seen in the correction curve in Fig. 4 is due primarily to the uncalibrated photoresponse of the handheld system.

As with Raman shift stretching, a linear regression analysis to third order in Raman shift wavenumber $k$ is used to quantify the amplitude ratio variation

$$\frac{I_{lab}}{I_{\Delta Nu}} = A_{lab} + B_{lab}k + C_{lab}k^2 + D_{lab}k^3 \tag{6}$$

The results for the regression analysis are given in Table III. The scaling of the laboratory spectra is accomplished by dividing the spectral data by the factor given in Eq. 6.

The adjusted $R^2$ statistic indicates that there is added

**TABLE II. Raman wavenumber shift corrections.**

| | Bruker wavenumber shift coefficients | Kaiser wavenumber shift coefficients |
|---|---|---|
| $a_{lab}$ | $5.3(2) \times 10^{1}$ | $6.4(2) \times 10^{1}$ |
| $b_{lab}$ | $-1.61(9) \times 10^{-1}$ | $-1.98(6) \times 10^{-1}$ |
| $c_{lab}$ | $1.6(1) \times 10^{-4}$ | $1.91(6) \times 10^{-4}$ |
| $d_{lab}$ | $-4.6(4) \times 10^{-8}$ | $-5.7(2) \times 10^{-8}$ |
| Adjusted $R^2$ | 0.89 | 0.98 |

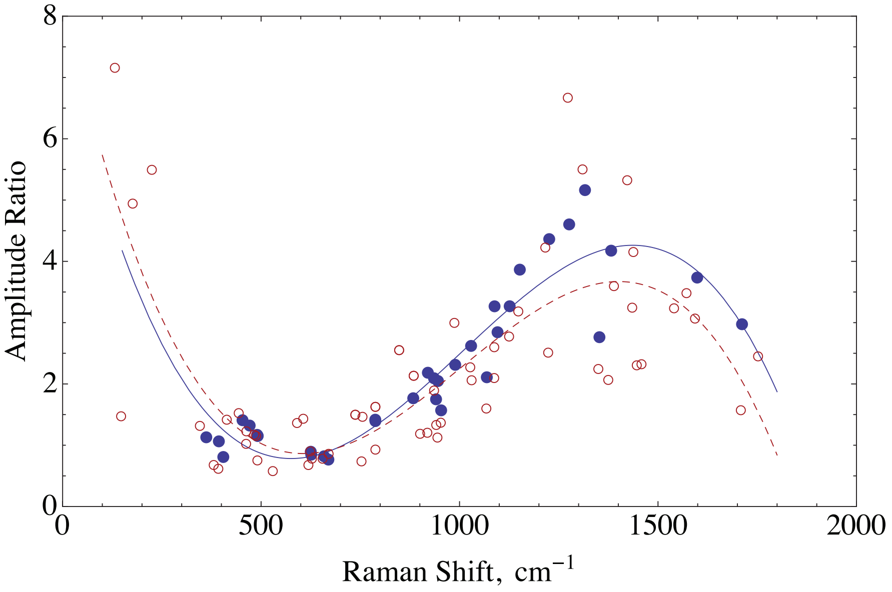

FIG. 4. Ratio of Raman line intensities for Bruker (open circles) and Kaiser (filled circles) relative to DeltaNu line intensities as a function of Raman shift. The dashed and solid lines are polynomial fits to Bruker and Kaiser line ratios, respectively.

variance not accounted for in the Bruker amplitude scaling. The likely reason for this added variance is that the Bruker fit used many additional lines that were not used in the Kaiser fit, and these lines might have been poorly suited for calibrating the intensity response. For example, in the Kaiser data the selection criteria limited the mapping study to larger amplitude lines; and, in fact, setting an amplitude threshold for selecting lines in the Bruker spectrum does reduce the scatter in the amplitude ratio data. In addition, the Bruker fitting included lines with Raman wavenumber shift $<400$ cm$^{-1}$, whereas the Kaiser fitting did not: these lines, in particular, are susceptible to baseline correction effects associated with the notch filter.

With the correction factor, the large systematic variation in line height is corrected; however, Fig. 4 shows that the line amplitudes in the adapted spectra are still uncertain by roughly 60%—this is the mean variance in amplitude ratio for the Kaiser mapping. This stochastic intensity error may be intrinsic to uncontrolled factors in the data collection. These uncontrolled factors include variable polarization cross sections in a solid sample that can change the intensity when the sample is reoriented;[8] laser heating that can affect the scattering cross section and is a possible issue with spectra collected with different wavelength lasers;[12,31] changes in Raman cross sections that occur with absorption in nonheterogeneous samples; pixel-to-pixel sensitivities across a two-dimensional CCD that add to the signal noise;[16] and differences in the instrument response relating to sample alignment, laser focus, and depth of focus.[8,15] Baseline correction methods, if they are used, may add to the stochastic error (e.g., see the discussion of Fig. 7 below). Thus, there may be limits to the management of line amplitudes in the spectra of handheld systems.

**Interpolation.** The final processing applied to the spectrum is to interpolate the spectra to the specific wavenumbers used by the DeltaNu system. This interpolation reduces the number of points in the finely delineated laboratory spectra to the 2001 point spectra used by DeltaNu. This reduction is accomplished by identifying the interval in the laboratory spectrum that contains the DeltaNu wavenumber and then applying a simple linear interpolation to find the spectral amplitude at the DeltaNu wavenumber.

## RESULTS

The success of adaptation of laboratory reference data into the DeltaNu material identification library was tested on a set of 10 chemicals. The spectra adapted from both the Bruker and Kaiser data were included in the DeltaNu library database. Other investigational libraries based on Kaiser data were added: these libraries involved conversions that left out some of the spectral corrections, as indicated in the Table IV. Data collected with the DeltaNu were evaluated against these adapted library spectra using the DeltaNu material identification "score" that the prototype displays in ranking possible matches. The material identification score is the HQI defined in Eq. 2. An HQI of 0.99 is an optimum match, and values $<0.99$ indicate decreasing correlation.

The two spectral libraries generated using all the algorithmic conversions described above are denoted as PNNL and TSL in Table IV, and they were scored with high correlation values by the DeltaNu material identification algorithm. The one exception is the TSL (Kaiser) conversion of calcium carbonate. While calcium carbonate shows mild fluorescence, the main issue affecting the score is the spectral mismatch at the lowest Raman shift, as shown in the inset of Fig. 5. This shortcoming of the conversion process could be improved by better sampling of mapping lines at low Raman shift.[14,15,24]

It is apparent from the scoring of TSL-0 (which was

**TABLE III. Raman amplitude scaling.**

| | Bruker amplitude coefficients | Kaiser amplitude coefficients |
|---|---|---|
| $A_{lab}$ | 8.2(9) | 8(1) |
| $B_{lab}$ | $-2.8(4) \times 10^{-2}$ | $-2.7(5) \times 10^{-2}$ |
| $C_{lab}$ | $3.3(4) \times 10^{-5}$ | $3.3(5) \times 10^{-5}$ |
| $D_{lab}$ | $-1.1(2) \times 10^{-8}$ | $-1.1(2) \times 10^{-8}$ |
| Adjusted $R^2$ | 0.55 | 0.86 |

**TABLE IV. Library testing.**

| | PNNL | TSL | TSL-2 | TSL-1 | TSL-0 | TSL-C |
|---|---|---|---|---|---|---|
| Baseline removal | NO | NO | NO | NO | NO | YES |
| Interpolation | YES | YES | YES | YES | YES | YES |
| Resolution broadening | YES | YES | YES | YES | NO | YES |
| Raman shift correction | YES | YES | YES | NO | NO | YES |
| Amplitude scaling | YES | YES | NO | NO | NO | YES |
| Acetone | 0.98 | 0.98 | 0.94 | 0.95 | 0.93 | 0.97 |
| Ammonium nitrate | 0.96 | 0.96 | 0.87 | 0.88 | 0.83 | 0.96 |
| Calcium carbonate | 0.97 | 0.82 | 0.81 | 0.61 | 0.56 | 0.82 |
| Ethanol | 0.97 | 0.98 | 0.95 | 0.93 | 0.90 | 0.97 |
| Isopropyl alcohol | 0.98 | 0.98 | 0.94 | 0.95 | 0.91 | 0.98 |
| Nitromethane | 0.96 | 0.96 | 0.89 | 0.87 | 0.78 | 0.96 |
| Sodium chlorate | 0.98 | 0.98 | 0.96 | 0.92 | 0.87 | 0.98 |
| Sugar, granulated | 0.96 | 0.94 | 0.82 | 0.68 | 0.63 | 0.94 |
| Sugar, powdered | 0.96 | 0.96 | 0.83 | 0.69 | 0.63 | 0.85 |
| Toluene | 0.94 | 0.97 | 0.74 | 0.68 | 0.66 | 0.95 |

processed only to interpolate to the number of data points) that unaltered spectra generally perform only marginally. Although the minimally processed acetone and isopropyl alcohol library entries score well, these spectra are dominated by single strong lines (e.g., see Fig. 6). It is also apparent that omitting one or more of the steps in the conversion procedure can lead to inferior results. Interestingly, removing the spectral background before converting the spectra (library TSL-C) does not seem to have a strong effect on the material identification score, nor does the illuminating laser wavelength. This weak effect seems to be true even for spectra displaying mild fluorescence, such as calcium carbonate in Fig. 5. Intensity error and fluorescence have only a weak influence on the HQI score of the adapted libraries. The reference spectra thus seem to be portable as long as they are wavelength and intensity calibrated.

## DISCUSSION AND CONCLUSIONS

Mapping functions were derived by comparing sets of spectra collected on selected materials by both laboratory and portable spectrometers.[8,12,13,15,16] The mapping functions enable the spectra of any material in the laboratory database to be converted into the portable database library. The method has the significant advantage of being able to update or augment commercial library databases with government-supplied data, obviating the expensive and time-consuming process of developing libraries for each system.

The example shown in Fig. 6 makes a comparison between the DeltaNu spectrum for acetone and the adapted library spectra based on the Bruker and the Kaiser data. The mapping shows good matching for both line positions and linewidths. The differenced spectra are shown in the inset to Fig. 6: these spectra are the Kaiser- and Bruker-based library spectra subtracted from the DeltaNu handheld spectrum. The differenced spectra are similar between the 785 and 1064 laboratory spectrometers, and the greatest departures in background are seen at the lowest wavenumber shifts and in the small fluorescence evident in the DeltaNu data. There are also evident inconsistencies in line amplitudes that remain after the amplitude scaling. Because the converted libraries demonstrated very high material identification scores despite the small amplitude incongruity, the line amplitude scaling applied here seems to be sufficiently accurate for this detection methodology. A similar insensitivity to the intensity correction was noted previously.[11]

It is not clear what more can be done to improve the intensity matching. It is known that variation in the relative peak amplitudes is the major inconsistency in spectral conversion between instruments.[8] The intensity mapping in this study was performed by comparing spectral data on identical samples for each instrument. An alternate approach is to calibrate each spectrometer with external intensity calibration standards such as calibrated irradiance sources or luminescent glass standards,[8,10,12] and correct the inconsistency in the calibrations.[11] Although these conventional techniques might improve on the standardization of the intensity calibration, they do not address the problem associated with the variability seen in the Raman spectra among materials. As long as the ensemble of calibration materials does not have a systematic intensity variance, the line

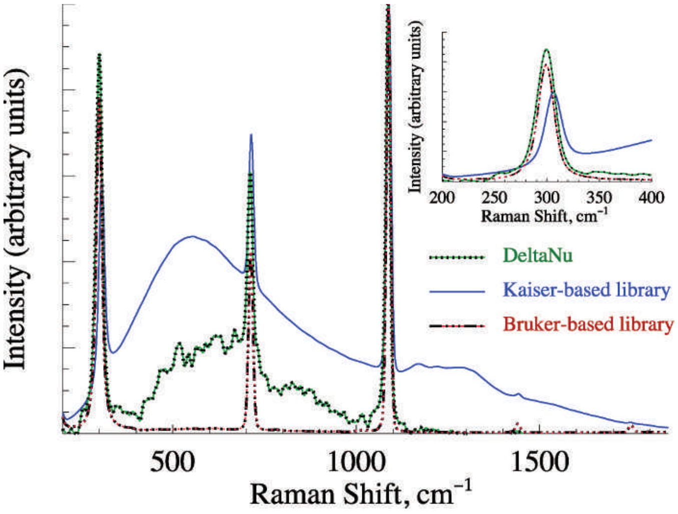

Fig. 5. Comparison of DeltaNu spectrum for calcium carbonate with the adapted Kaiser-based spectrum. The inset is an expanded view of the low Raman-shift line.

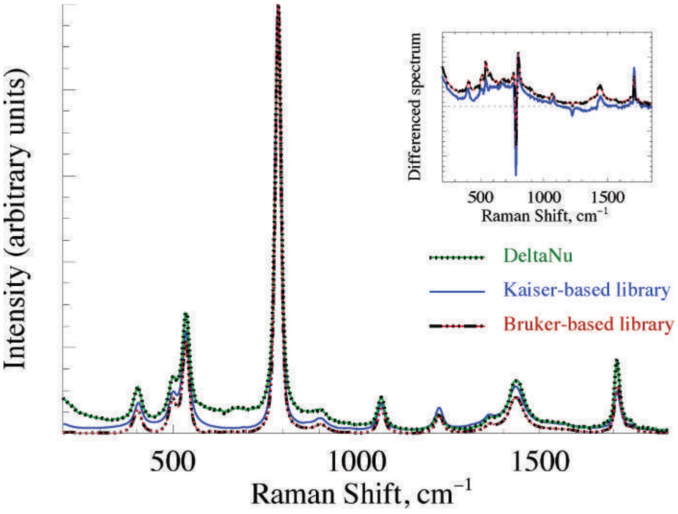

Fig. 6. Comparison of DeltaNu spectrum for acetone with the adapted library spectra. The inset shows a differenced spectrum for each library (the y-scale is expanded eightfold).

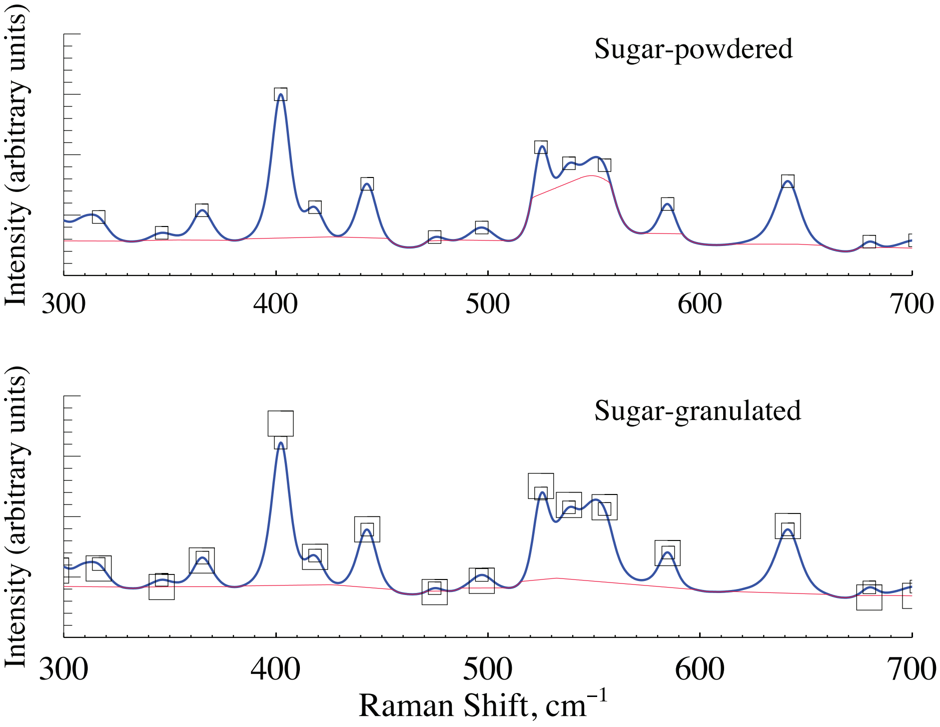

FIG. 7. Wavelet analysis of the Kaiser powdered sugar and granulated sugar spectra is compared. The baseline is plotted along with markers showing the wavelet peak solutions. On the bottom figure, the wavelet peaks from upper solution are plotted with oversize markers for comparison.

sampling used in this article should produce a similar intensity mapping as the calibration standards.

The instrument-to-instrument comparison also was used for the important wavenumber matching. The calibration materials were selected to have well-sampled spectral coverage between 300 and 1850 cm$^{-1}$, but other chemicals or additional chemicals can be added to the calibration. One clear recommendation for future work is to sample better the low and high wavenumber shift ranges to constrain the scaling at the ends of the spectra; problems in the extreme ends of the spectra were clearly seen to cause problems in the HQI score, as illustrated by the spectrum in Fig. 5.

The algorithms used for automated baseline correction and peak identification were found to be useful in the spectral analysis, but not without potential pitfall. An example is the case of powdered sugar, where applying a baseline correction to the spectrum produced a poorly performing library spectrum relative to the uncorrected TSL spectrum (see Table IV). Figure 7 shows that the automated baseline solution for powdered sugar was different from the solution for granulated sugar in the wavenumber region near 540 cm$^{-1}$ where superimposed lines produce a broadened response, and this seems to be the difference in how the respective baseline-corrected library spectra performed. However, in our work, the baseline correction does not seem to produce improvement in library performance for reasons other than the efficacy of the baseline solution.

In conclusion, testing as part of this study shows that user-created libraries for the DeltaNu prototype spectrometer worked well with the identification algorithm for matching spectra. This relationship was demonstrated with user libraries derived from NIR laboratory spectrometers with two different wavelength lasers. This finding indicates that differences in spectra between two NIR spectrometers—a laboratory spectrometer and a portable spectrometer—can be quantified and corrected to enable detection on any of several different portable systems, assuming the reference data are at higher resolution and are accurately calibrated and vetted. The results support the strategy of collecting Raman databases on laboratory spectrometers for adaptation into libraries on fielded systems. Additional study is underway to determine whether this methodology can be successful over a broad range of materials and with other portable spectrometers.

Finally, this work has shown that, within the scope of study, data can be ported between different NIR wavelengths, which may not necessarily be the case for visible or ultraviolet wavelengths. In the visible or ultraviolet, where Raman scattering is greater by the $\nu^4$ efficiency factor, resonance or preresonance enhancement of differing bands could play a role for certain species.[21,32]

## ACKNOWLEDGMENTS

This work was supported by Technical Support Working Group contract N41756-04-D-4245. Carolyn S. Brauer is supported in part by an appointment to the Transportation Security Laboratory Visiting Science Program administered by the Oak Ridge Institute for Science and Education (ORISE) through an interagency agreement between the U.S. Department of Energy (DOE) and the U.S. Department of Homeland Security (DHS). ORISE is managed by Oak Ridge Associated Universities (ORAU) under DOE contract DE-AC05-06OR23100. All opinions expressed in this paper are the authors' opinions and do not necessarily reflect the policies and views of DHS, Transportation Security Laboratory, DOE, or ORAU/ORISE.

---

1. P. Vandenabeele. "Raman Spectroscopy". Anal. Bioanal. Chem. 2010. 397: 2629-2630.
2. D. Moore, R. Scharff. "Portable Raman Explosives Detection". Anal. Bioanal. Chem. 2009. 393: 1571-1578.
3. P. Vandenabeele, K. Castro, M. Hargreaves, L. Moens, J. Madariaga, H. Edwards. "Comparative Study of Mobile Raman Instrumentation for Art Analysis". Anal. Chim. Acta. 2007. 588: 108-116.

4. J. Jehlicka, A. Culka, P. Vandenabeele, H.G. Edwards. "Critical Evaluation of a Handheld Raman Spectrometer with Near Infrared (785 nm) Excitation for Field Identification of Minerals". Spectrochim. Acta, Part A. 2011. 80(1): 36-40.
5. S.J. Kelloway, N. Kononenko, R. Torrence, E.A. Carter. "Assessing the Viability of Portable Raman Spectroscopy for Determining the Geological Source of Obsidian". Vib. Spectrosc. 2010. 53(1): 88-96.
6. L. Borland, M. Brickhouse, T. Thomas, A. Fountain. "Review of Chemical Signature Databases". Anal. Bioanal. Chem. 2010. 397: 1019-1028.
7. A.W. Fountain III, J.A. Guicheteau, W.F. Pearman, T.H. Chyba, S.D. Christesen. "Long-Range Standoff Detection of Chemical, Biological, and Explosive Hazards on Surfaces". In: T. George, M.S. Islam, A.K. Dutta, editors. Micro- and Nanotechnology Sensors, Systems, and Applications II. Proc. SPIE, 2010. 7679(1), Pp. 76790H-76803H.
8. R. McCreery. "Photometric Standards for Raman Spectroscopy". In: J. Chalmers, P. Griffiths, editors. Handbook of Vibrational Spectroscopy. Chichester, UK: John Wiley and Sons, 2002. Pp. 920-932.
9. D. Moore. "Long-Term Data Archiving". Anal. Bioanal. Chem. 2010. 396: 189-192.
10. T.J. Johnson, Y.-F. Su, K.H. Jarman, B.M. Kunkel, J.C. Birnbaum, A.G. Joly, E.G. Stephan, R.G. Tonkyn, R.G. Ewing. "Demonstrated Wavelength Portability of Raman Reference Data for Explosives and Chemical Detection". Int. J. Spectrosc. 2012. 297056: 1-11.
11. J.D. Rodriguez, B.J. Westenberger, L.F. Buhse, J.F. Kauffman. "Standardization of Raman Spectra for Transfer of Spectral Libraries across Different Instruments". Analyst. 2011. 136(20): 4232-4240.
12. S.J. Choquette, E.S. Etz, W.S. Hurst, D.H. Blackburn, S.D. Leigh. "Relative Intensity Correction of Raman Spectrometers: NIST SRMs 2241 through 2243 for 785 nm, 532 nm, and 488 nm/514.5 nm Excitation". Appl. Spectrosc. 2007. 61: 117-129.
13. A.W. Fountain, C.K. Mann, T.J. Vickers. "Routine Wavenumber Calibration of an FT-Raman Spectrometer". Appl. Spectrosc. 1995. 49: 1048-1053.
14. A.W. Fountain, T.J. Vickers, C.K. Mann. "Factors That Affect the Accuracy of Raman Shift Measurements on Multichannel Spectrometers". Appl. Spectrosc. 1998. 52: 462-468.
15. D. Hutsebaut, P. Vandenabeele, L. Moens. "Evaluation of an Accurate Calibration and Spectral Standardization Procedure for Raman Spectroscopy". Analyst. 2005. 130: 1204-1214.
16. W.S. Hurst, S.J. Choquette, E.S. Etz. "Requirements for Relative Intensity Correction of Raman Spectra Obtained by Column-Summing Charge-Coupled Device Data". Appl. Spectrosc. 2007. 61: 694-700.
17. E.D. Emmons. A.W. Fountain III, J.A. Guicheteau, S.D. Christesen. "Comparison of Absolute Raman Cross Sections of Explosives in the Solid State and in Solution". In: P.M. Champion, L.D. Ziegler, editors. Proceedings of the XXII International Conference on Raman Spectroscopy. AIP Conf. Proc. 2010. 1267(1), Pp. 508-509.
18. M.L. Lewis, I.R. Lewis, P.R. Griffiths. "Raman Spectrometry of Explosives with a No-Moving-Parts Fiber Coupled Spectrometer: A Comparison of Excitation Wavelength". Vib. Spectrosc. 2005. 38: 17-28.
19. S. Nunn, K. Nishikida. "Advanced ATR Correction Algorithm". Thermo Electron Corporation Application Note 1153. 2003. http://www.thermoscientific.com [accessed Jun 6 2012].
20. Bruker Optik GmbH. "Bruker IFS 66v/S Spectrometer, User's Manual". 1998.
21. S.D. Williams, T.J. Johnson, T.P. Gibbons, C.L. Kitchens. "Relative Raman intensities in $C_6H_6$, $C_6D_6$, and $C_6F_6$: A Comparison of Different Computational Methods". Theor. Chem. Acc. 2007. 117: 283-290.
22. Kaiser Optical Systems, Inc. "RamanRxn1 Operations Manual". 2004.
23. A. Kwiatkowski, M. Gnyba, J. Smulko, P. Wierzba. "Algorithms of Chemical Detection Using Raman Spectra". Metrol. Meas. Syst. 2010. XVII(4): 549-560.
24. A.W. Fountain. "Abscissa Calibration and Transfer for the Development of Instrument Independent Raman Spectra". Ph.D. Thesis. Ft. Lauderdale, FL: Florida State University ,1997.
25. D. Moore. "Recent Advances in Trace Explosives Detection Instrumentation". Sens. Imaging. 2007. 8: 9-38.
26. W.F. Pearman, A.W. Fountain. "Classification of Chemical and Biological Warfare Agent Simulants by Surface-Enhanced Raman Spectroscopy and Multivariate Statistical Techniques". Appl. Spectrosc. 2006. 60: 356-365.
27. K. Hornik. "The R FAQ". 2011. http://CRAN.R-project.org/doc/FAQ/R-FAQ.html. [accessed Jun 26 2011].
28. Z.-M. Zhang, S. Chen, Y.-Z. Liang, Z.-X. Liu, Q.-M. Zhang, L.-X. Ding, F. Ye, H. Zhou. "An Intelligent Background-Correction Algorithm for Highly Fluorescent Samples in Raman Spectroscopy". J. Raman Spectrosc. 2010. 41(6): 659-669.
29. A. Tripathi, E.D. Emmons, P.G. Wilcox, J.A. Guicheteau, D.K. Emge, S.D. Christesen, A.W. Fountain III. "Semi-Automated Detection of Trace Explosives in Fingerprints on Strongly Interfering Surfaces with Raman Chemical Imaging". Appl. Spectrosc .2011. 65(6): 611-619.
30. Wolfram Research, Inc. "Mathematica Edition". Version 8.0. 2010.
31. T.J. Vickers, C.K. Mann, C.-H. Tseng. "Changes in Raman Spectra Due to Near-IR Excitation". Appl. Spectrosc. 1992. 46: 1200-1202.
32. S. Wallin, A. Pettersson, H. Östmark, A. Hobro. "Laser-Based Standoff Detection of Explosives: A Critical Review". Anal. Bioanal. Chem. 2009. 395: 259-274.